CMU Journal of Science
The Official Scientific Journal of Central Mindanao University
ISSN Print: 0116-7847 js.cmu.edu.ph ISSN Online: 2704-3703

Research Article

GIS-Based Multi-Criteria Decision Analysis for Retarding Basin Site Selection in Bukidnon, Philippines with Pre- and Post-Retardation Analysis

Analou A. Vicente[1], Kay Q. Abarquez[1], Jemima R. Perodes[1]*,

[1] Department of Civil Engineering, Central Mindanao University; s.vicente.analou@cmu.edu.ph; s.abarquez.kay@cmu.edu.ph; f.jemima.perodes@cmu.edu.ph

Citation: Vicente, A.A., Abarquez, K.Q., & Perodes, J.R. (2024). *"GIS-Based Multi-Criteria Decision Analysis for Retarding Basin Site Selection in Bukidnon, Philippines with Pre- and Post-Retardation Analysis."* CMU Journal of Science. 28(2), 63

Academic Editor: Dr. Ma Bernadeth Lim

Received: November 03, 2024
Revised: December 04. 2024
Accepted: December 13, 2024
Published: December 27, 2024

ABSTRACT

This study presents a spatial-based approach to identifying locations for retarding basins and assesses their impact on design discharges in areas prone to riverine flooding. A decision framework integrating multiple criteria, weighted by the analytical hierarchy process (AHP) and generated through geographic information system, is applied in the Taganibong watershed, Bukidnon, Philippines. Criteria such as land use/cover (36%), drainage proximity (27%), watershed slope (20%), infiltration capacity (6%), soil type (6%), and road proximity (5%) are considered. The resulting overlay map delineates areas that are highly suitable (0.67%), moderately suitable (57.76%), suitable (39.58%), and not suitable (2.00%) for retarding basin placement. Three prospective sites were identified based on coherence with suitability and flood inundation maps. HEC-HMS was used to assess the impact of having a retarding basin at these locations on design discharges in the Taganibong Creek. The model gained favorable calibration (NSE: 0.718, RSR: 0.5, PBIAS: -9.1) and validation (NSE: 0.685, RSR: 0.6, PBIAS: -4.85) results. Simulations were performed for different scenarios which produced significant peak discharge reductions (RB1: 75%, RB2: 77%, RB3: 13%) and peak time delays (RB1: 1.5 hours, RB2: 2 hours, RB3: 0.25 hours). RB2 emerges as the most suitable location.

Keywords: geographic information system, multi-criteria decision analysis, analytical hierarchy process, land suitability, retarding basin

1. INTRODUCTION

The environment comprises resources and hazards [1], and interactions between natural landscapes and human activities can transform resources into hazards. At Taganibong Creek, flooding issues trace back to a diversion canal created in the late 1970s to supply water during dry seasons by rerouting flows from Kulaman River [2]. Over time, this canal expanded which allowed excess discharge to spill into Taganibong Creek and consequently causing frequent flooding in Musuan plain. In 2012, Central Mindanao University proposed a dam to close the canal [2], but jurisdictional limits delayed action. A recent flood on August 5, 2022, which inundated parts of Dologon, Maramag, Bukidnon, further demonstrated the pressing need for intervention.

To mitigate flood effectively, strategic site selection and appropriate mechanisms to control peak discharge are essential. One common approach is the use of retarding or detention basins, which store excess water to reduce downstream flooding. Optimal sites for these structures are ideally located upstream to protect downstream areas [3]. Due to limited land availability and complex site requirements, Geographic Information System (GIS) combined with Multi-Criteria Decision Analysis (MCDA) can identify suitable locations by balancing diverse criteria.

MCDA helps resolve conflicting objectives by simplifying decision components and synthesizing them into actionable insights [5]. Among various methods, the AHP is widely used due to its ease of integration with GIS and reliable criteria weighing [7, 8]. Prior research has utilized GIS-MCDA for flood zoning, hazard mapping, and siting retention ponds [9-14], yet limited studies address retarding basin placement, particularly in rural or smaller watersheds.

This study addresses this gap by applying GIS-based MCDA and hydrological modeling to identify optimal sites for a retarding basin in Taganibong Creek. The study will determine criteria weights, generate a suitability map, and simulate impacts on peak discharge and delay using HEC-HMS.

2. METHODOLOGY

2.1 Study area

The total area of the upstream Taganibong catchment basin is 44.18 km^2, shown in Fig. 1, comprising the Central Mindanao University land domain and a few portions of barangays Guinoyoran and Tugaya in Valencia City and Dologon in Maramag. The outlet of the study area is located at 125.064 degrees longitude and 7.85698 degrees latitude (WGS 84). Elevation within the watershed ranges from 300 to 1000 meters above mean sea level.

The soil type in Bukidnon varies from clay loam to rough and stony land [18]. In the CMU land domain, the academic campus, forestland, and agricultural land account for 4.76, 39.28, and 55.95% of the total land cover, respectively [19].

Based on the climate map of the Philippines generated by the Philippine Atmospheric, Geophysical and Astronomical Services Administration (PAGASA), the study area has a type III climate. The area has no very pronounced maximum rainfall period with a dry season from November to April and wet for the rest of the year.

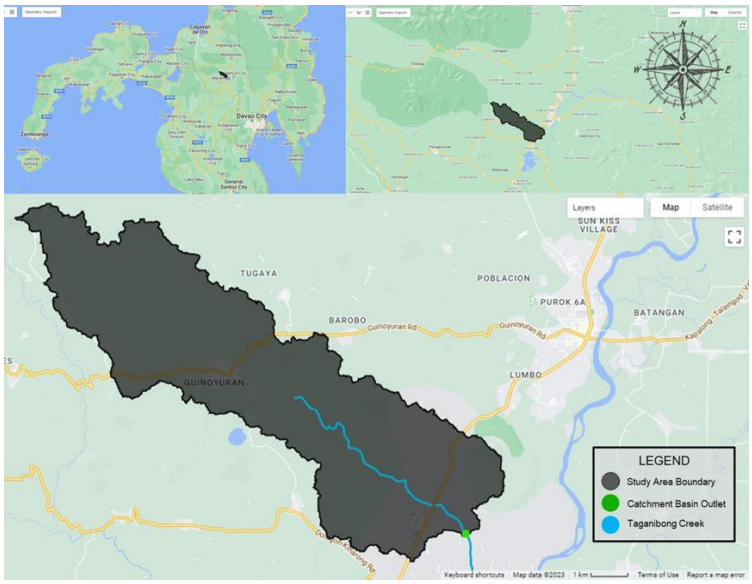

Fig. 1. Upstream Taganibong catchment basin with outlet near PAGASA-Agrometeorology Station.

2.2 Conceptual framework

Identifying suitable areas to attenuate peak flood discharge and delay peak time requires a framework involving location prospecting and hydrological modeling, shown in Fig. 2. The location prospecting phase plays a crucial role in identifying appropriate sites for the retarding basin using the GIS-based AHP. Simultaneously, the hydrological modeling using HEC-HMS assesses which area would be most effective in reducing peak flood discharge.

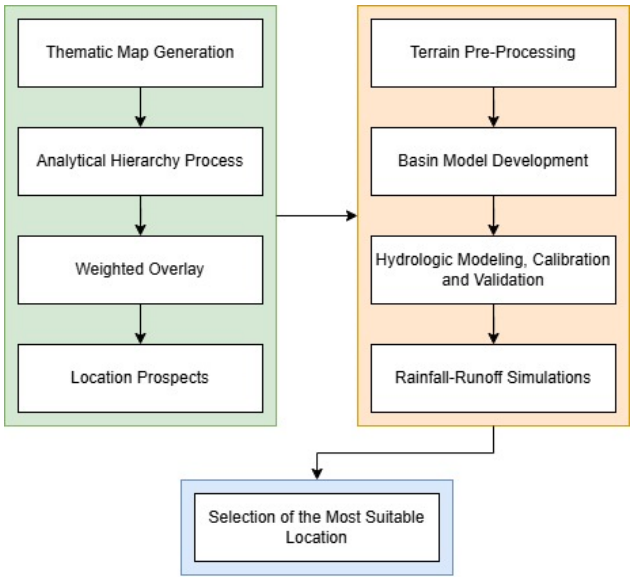

Fig. 2. Procedural Framework

2.3 Analytical Hierarchy Process

AHP is a structured model that deals with complex decisions. Contrary to selecting a correct choice, this decision-making framework identifies the one that best suits the needs. Alongside underlying information, human judgment is crucial in performing the evaluations. Its goal is to designate weight among the criteria identified, evaluating each according to the intensity of suitability.

The first level is defining the problem, which is to locate suitable sites for a retarding basin along upstream Taganibong Creek. The second level is predetermining the main criteria in selecting suitable areas for a retarding basin. The third level is identifying sub-criteria of each main criterion. The last level is associating these sub-criteria to each apt degree of suitability using preference values (PV)—zero being the least suitable and five being the most suitable, as shown in Fig. 3.

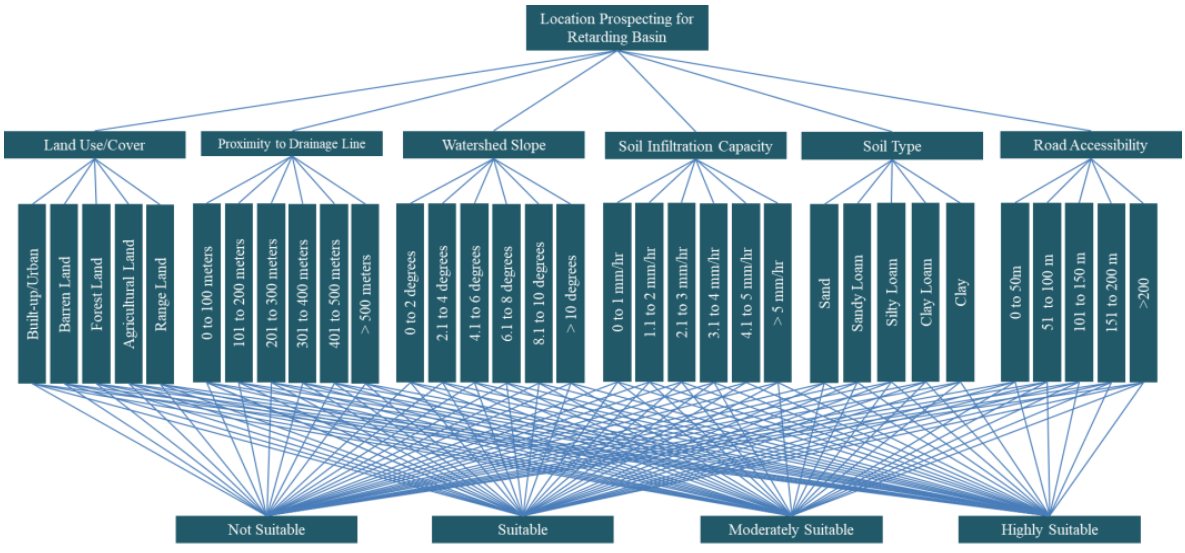

Fig. 3. AHP model for retarding basin location prospecting [20].

Six main criteria are pre-identified: land use/cover, proximity to drainage line, watershed slope, soil infiltration capacity, soil type, and road accessibility. Land use/cover is one of the criteria, as retarding basins are suitable for land with little to no clearing works. Proximity to the drainage line is also best considered because water flow accumulates along this line, thus collecting a greater volume. The watershed slope allows natural water impediments for storage. Soil type and infiltration must be taken into account, as well, to recharge the stored overflow flood discharge to the ground naturally. Road accessibility is practically for ease of construction and maintenance. Thematic maps for each criterion mentioned were generated using GIS software.

Additionally, to get each thematic map's weight or degree percentage, a pairwise comparison (n x n matrix) was created, n being the main criterion. These criteria were evaluated relative to one another using a standard scale of relative importance based on Table 1. A normalized pairwise comparison matrix was derived by simply getting the ratio of each original pairwise value to the sum of each column value. By getting the ratio of the sum of the row to the number of criteria, criterion weight was derived.

Table 1. The fundamental scale for pairwise comparison in the analytic hierarchy process [21].

Intensity of Importance	Definition	Explanation
1	Equal importance	Two activities contribute equally to the objective
3	Moderate importance of one over another	Experience and judgment slightly favor one activity over another
5	Essential or strong importance	Experience and judgment strongly favor one activity over another
7	Very strong importance	An activity is favored very strongly over another; its dominance demonstrated in practice
9	Extreme importance	The evidence favoring one activity over another is of the highest possible order of affirmation
2,4,6,8	Intermediate values between the two adjacent judgments	When compromise is needed
$\frac{1}{2}', \frac{1}{3}', \frac{1}{4}', \frac{1}{5}', \frac{1}{6}', \frac{1}{7}', \frac{1}{8}', \frac{1}{9}$	Reciprocals	If activity a has one of the above numbers assigned to it when compared with activity j, then j has the reciprocal value when compared with i

Consistency Ratio (CR) was used to check the accuracy of the weights derived. The Consistency Index (CI) to Random Index (RI) ratio was used. CI is the difference ratio of the largest eigenvalue (λ) and the number of criteria (n) to n minus 1. Meanwhile, RI is the consistency index of a randomly produced pairwise comparison matrix, as shown in Table 2. Weight accuracy lies on CR values lesser than 0.10.

Table 2. Consistency indices for a randomly generated matrix [22].

n	2	3	4	5	6	7	8
RI	0.00	0.52	0.89	1.11	1.25	1.35	1.40

2.4 Thematic map generation for weighted overlay

Generation of thematic maps for each criterion in this study utilizes satellite imagery, digital terrain model (DTM), soil map, and road spectral layer with sources and details indicated in Table 3. The maps were reclassified using GIS software. These thematic maps were then overlaid using the weight criteria of each factor derived using AHP.

Table 3. Data utilized for thematic map generation

Data	Details/ Description	Source	Extracted/ Generated Layer(s)	Data Type
Satellite Imagery	Red, Green, Blue, and near-infrared bands with 10 m by 10m resolution	Sentinel-2, EU Copernicus Programme	Land Use/Cover Map	raster
			Soil Infiltration Capacity	raster
Digital Elevation Model (DTM)	DTM with 1 m by 1 m resolution, format: TIFF	Department of Science and Technology, Phil-LiDAR Program	Watershed slope	raster
			Proximity to drainage line (through Euclidean distance)	raster
Soil Map	Soil Map of Maramag and Valencia City	Municipal Planning and Development Office – Maramag, Valencia City	-	vector
Road Spectral Layer		Open Street Map	Proximity to road	vector

PVs are assigned to each map and reclassified with ranges of suitability indicated in Table 4, which corresponds to the third-level sub-criteria. These preference values were used to unify the weighted overlay map.

Table 4. Preference values range.

Preference values	Description
$0<PV\leq1$	Not Suitable
$1<PV\leq2$	Suitable
$2<PV\leq4$	Moderately Suitable
$4<PV\leq5$	Highly Suitable

2.4.1 Land use/cover

The land use land cover (LULC) map of the study area was generated using remotely sensed images. Two images were retrieved from Sentinel-2, with cloud covering less than 10%. The image with the most minor cloud covering was considered. A near-natural color composite band was created and masked by the area of interest or the Taganibong watershed polygon. Training samples in each LULC category were extracted with enabled base maps for visual reference and were merged into a signature file. Support Vector Machine Training (SVM) was used to classify the composite band into LULC and further assessed for accuracy and reclassified with its corresponding preference values, as shown in Table 5. Support vector machines are computational algorithms that find the best separation hyperplane, one that provides the maximized margin distance between nearest points of the two classes. Compared to other classifiers, SVM are robust, accurate and

very effective even when training samples is small and not linearly separable, posing a greater likelihood of generating good classifiers [23].

Table 5. Preference values for LULC.

LULC category	Preference Value
Urban/Built-up	0
Barren Land	2
Forestland	3
Agricultural Land	4
Rangeland	5

2.4.2 Drainage proximity

Prior to drainage proximity map generation, the 1-m resolution DTM was subjected to watershed delineation utilizing the Hydrology Tools in ArcGIS. With a defined projection, DTM was subjected to fill, sink, flow direction, flow accumulation, outlet placement, watershed delineation, defined streams, and watershed and stream raster, which were converted to vectors. With stream vector as input, under spatial analyst tools, Euclidean distance was utilized to reclassify the map according to proximity to the drainage line into six classes with specified distances indicated in Table 6.

Table 6. Preference values for drainage proximity.

Distance from drainage line (meters)	Preference Value
0<distance≤100	5
101<distance≤200	4
201<distance≤300	3
301<distance≤400	2
401<distance≤500	1
>500	0

2.4.3 Watershed slope

The watershed slope map was generated from a 1-m resolution DTM with a defined projection and was used as input for the fill tool. The filled raster was further used as input in the slope tool, generating watershed slopes with six reclassified classes with corresponding range values indicated in Table 7.

Table 7. Preference values for watershed slope.

Slope range (degrees)	Preference Value
0 < slope ≤ 2	5
2 < slope ≤ 4	4
4 < slope ≤ 6	3
6 < slope ≤ 8	2
8 < slope ≤ 10	1
slope < 10	0

2.4.4 Infiltration capacity

An infiltration capacity map was generated by assigning infiltration capacity values to the LULC raster. Prior to map generation, double-ring infiltrometer tests were conducted on each type of soil in the area. For one type of soil, infiltration capacity tests were held for each identified LULC category. The infiltration capacity raster was reclassified, assigning preference values indicated in Table 8.

Table 8. Preference values for infiltration capacity.

Infiltration capacity (inf) range (cm/hr)	Preference Value
0 < inf ≤ 1	0
1 < inf ≤ 2	1
2 < inf ≤ 3	2
3 < inf ≤ 4	3
4 < inf ≤ 5	4
inf > 5	5

2.4.5 Soil type

The soil map was generated from a polygon feature class. The soil polygon was converted into a raster file, and the number of classes was reclassified using the preference values indicated in Table 9.

Table 9. Preference values for each soil type

Soil type	Preference Value
Sand	5
Sandy loam	4
Silty loam	3
Clay loam	2
Clay	1

2.4.6 Proximity to road

Distance to the road raster was generated from the exported road spectral map of the study area from OpenStreetMap. With road spectral vector as input, under spatial analyst tools, Euclidean distance was utilized to reclassify the map according to proximity to the road network into six classes with specified distances indicated in Table 10.

Table 10. Preference values for road accessibility.

Proximity to road (m)	Preference Value
0<distance≤50	5
50<distance≤100	4
100<distance≤150	3
150<distance≤200	2
> 200	1

2.5 Weighted overlay

Thematic maps generated for the six criteria considered were overlaid with criterion weights calculated using the AHP by pairwise comparison matrix. The area of each suitability zone category was calculated.

2.6 Location prospects

Based on the weighted overlay map, suitable locations for retarding basins were identified. A simulated 6-hour 25-year design flood was used for flood inundation map generation. Inundation depths due to overflow discharge were quantified and compared on the overlay map, identifying regions of accord.

2.7 Hydrologic Modeling in HEC-HMS

To study the effectiveness of the prospect retarding basins in lowering the peak flow and delaying time to peak, rainfall-runoff analyses were performed for the Taganibong watershed with and without the retarding basins and at various rainfall return periods. The process is shown in Fig. 4.

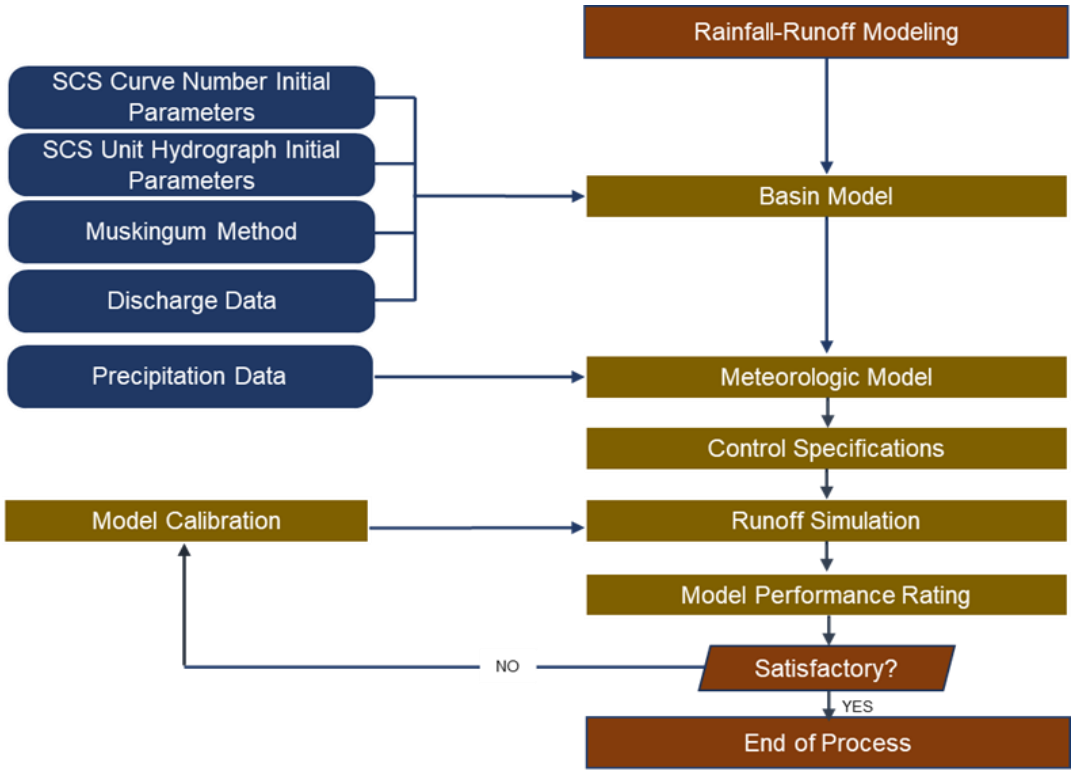

Fig. 4. Rainfall-Runoff Modeling in HEC-HMS [20].

2.7.1 Terrain Preprocessing

The 1-m-resolution digital elevation model (DEM) terrain was set to the WGS 84/UTM Zone 51N coordinate system and integrated into the basin model. Key preprocessing steps included handling terrain depressions by generating sink fill and sink location datasets and managing water movement through generating flow direction and flow accumulation layers. The process also involved identifying stream networks based on a minimum drainage area threshold of 0.6 sq. km, delineating watershed elements using GIS tools, and defining specific parameters like the percent impervious field and initial abstraction.

2.7.2 Model Development

The watershed elements, comprising subbasins and reaches, were delineated after identifying the breakpoint or outlet. The designated outlet point for the study area is at a latitude of 7.85698 and a longitude of

125.064 degrees. The model encompasses a total of 10 subbasins and 9 reaches.

The model employed the Soil Conservation Service (SCS) curve number for loss calculation, the SCS unit hydrograph for rainfall-runoff transformation, and the Muskingum method for reach routing. Initial values for various parameters, including loss, transform, and routing parameters, were input into the basin model.

The loss model based on the SCS curve number method requires the availability of initial abstraction data, curve number data, and percent impervious data for each subbasin within the basin model [24]. By applying the SCS curve number loss model, the excess precipitation P_e can be calculated using Equation (1).

$$P_e = \frac{(P-I_a)^2}{P-I_a-S} \tag{1}$$

P_e is the precipitation data, Ia is the initial abstraction calculated in Equation (2), and S is the maximum potential retention utilizing SI unit, calculated in Equation (3) where CN is the curve number estimated using hydrologic soil-cover complex data.

$$I_a = 0.2S \tag{2}$$

$$S = 254(\frac{100}{CN} - 1) \tag{3}$$

The transform model utilized was the SCS unit hydrograph which requires only the unit hydrograph lag time, estimated using Equation (4):

$$t_{lag} = 0.6T_c \tag{4}$$

where T_c is the time of concentration, or the time taken by a rainfall drop to travel from the farthest point in the watershed to the outlet. Tc will be calculated using equation (5):

$$T_c = \frac{l^{0.8}(S+1)^{0.7}}{1140Y^{0.5}} \tag{5}$$

where l is the flow length (h), S is the maximum potential retention, and Y is the average watershed land slope (%).

The parameters for the Muskingum method for routing reaches are assumed and initially assigned to all reaches as follows: a Muskingum K value of 0.5 and a Muskingum X value of 0.25.

The meteorological model used the Specified Hyetograph method to estimate precipitation, which relies on time-series data that detail precipitation over specific time periods. To generate this data, basin-averaged precipitation from a single gauge to represent the entire subbasin was used.

2.7.3 Model Calibration and Validation

A calibration process was carried out to improve the accuracy of the model's predictions. Specific parameters of the model were adjusted to align the simulated runoff more closely with the observed discharge data and consequently enhance the overall performance and accuracy of the model. The simulation for calibration started at 7:00 AM on December 4, 2012 [33], and ended at 00:30 AM on December 5, 2012, at 15-minute intervals. Moreover, to further validate the prediction performance of the model, a simulation was performed for a rainfall event that started at 3:00 PM on August 16, 2016 [34] and ended at 2:00 AM on August 17, 2016, at 10-minute intervals.

2.7.4 Model Performance Rating

To evaluate the performance of the rainfall-runoff model, the Nash-Sutcliffe efficiency (NSE) shown in Equation (6), percent bias (PBIAS) shown in Equation (7), and root mean square-standard deviation ratio (RSR) shown in Equation (8) were calculated. The NSE is a commonly used metric for assessing the accuracy of hydrological models. It measures the agreement between observed and simulated discharge values, quantitatively measuring the model's performance in replicating the observed hydrological behavior. A model's performance rating depends on the calculated values for NSE, RSR, and PBIAS at a certain range, as shown in Table 11.

$$NSE = 1 - \left[\frac{\Sigma_{i=1}^{n}(Y_i^{obs}-Y_i^{sim})^2}{\Sigma_{i=1}^{n}(Y_i^{obs}-Y_i^{mean})^2}\right] \tag{6}$$

$$PBIAS = \frac{\Sigma_{i=1}^{n}(Y_i^{obs}-Y_i^{sim})\cdot 100}{\Sigma_{i=1}^{n}Y_i^{obs}} \tag{7}$$

$$RSR = \frac{\sqrt{\Sigma_{i=1}^{n}(Y_i^{obs}-Y_i^{sim})^2}}{\sqrt{\Sigma_{i=1}^{n}(Y_i^{obs}-Y_i^{mean})^2}} \tag{8}$$

where Y_i^{obs} is the observed flow, Y_i^{sim} is the simulated flow, and Y_i^{mean} is the average of the observed flow.

Table 11. Model performance rating adapted [25].

Performance Rating	NSE	RSR	PBIAS
Very Good	$0.75 \leq NSE \leq 1.00$	$0.00 \leq RSR \leq 0.50$	$\|PBIAS\| < 10$
Good	$0.65 < NSE \leq 0.75$	$0.50 < RSR \leq 0.60$	$10 < \|PBIAS\| \leq 15$
Satisfactory	$0.50 < NSE \leq 0.65$	$0.60 \leq RSR \leq 0.70$	$15 < \|PBIAS\| \leq 25$
Unsatisfactory	$NSE < 0.50$	$RSR > 0.70$	$\|PBIAS\| > 25$

2.7.5 Runoff simulations

To determine the optimal location for a retarding basin in the Taganibong Creek catchment, the validated hydrological model was used to visualize the response of the watershed with and without the presence of such a retarding basin. The simulation runs were for 3-hour, 6-hour, 10-hour, and 24-hour rainfall events with 10-year, 25-year, 50-year, and 100-year return periods. The input rainfall hyetographs were produced from the rainfall intensity-duration-frequency (IDF) data sourced from the Malaybalay Synoptic Station of PAGASA [30-32]. Runoff hydrographs were then generated, considering scenarios both with and without the implementation of a retarding basin at the aforementioned various rainfall durations and return periods.

2.8 Reservoir Routing and Storage Methods

The reservoir discharge was represented using the level pool or Modified Puls routing model which divides the entire analysis period into uniform intervals of duration t and iteratively addresses a one-dimensional approximation of the continuity equation in Equation (9):

$$I_{avg} - O_{avg} = \frac{\Delta S}{\Delta t} \tag{9}$$

where I_{avg} is the average inflow during a time interval; O_{avg} is the average outflow during the time interval; ΔS is the storage change.

In this study, the outflow structures reservoir routing method was utilized as it is designed to model reservoirs with several uncontrolled outlet structures, while the elevation-area method was used as the storage method. Equation (10) expresses the conic formula used to approximate storage [24]:

$$\Delta S = \frac{(elev_1 - elev_2)}{3}(A_1 + A_2 + \sqrt{A_1 A_2}) \tag{10}$$

where ΔS is the incremental storage between two reservoir elevations, $elev_1$ and $elev_2$, and their respective sectional areas are A_1 and A_2. One drawback of this method is its limited applicability to massive reservoirs, where the assumption of a level pool is unrealistic. For the initial condition, inflow is configured as equal to outflow. This means that the reservoir's inflow at the beginning of the simulation is utilized, and the storage-discharge curve is employed to calculate the necessary storage to produce an equivalent flow rate to the outflow from the reservoir [24].

2.9 Selecting Location for Retarding Basin

The optimal site for the retarding basin was determined based on the reduction of peak flow rates, as identified by the validated hydrological model comparing scenarios with and without the basin. The location that demonstrated the greatest decrease in peak flow was chosen for the retarding basin.

3. RESULTS AND DISCUSSION

3.1 Criteria weights

By pairwise comparison matrix, shown in Table 12, criteria are paired, row by column, and evaluated based on their relative importance. Diagonal values equate to one since one factor is equally essential to itself. LULC is immediately not equal nor of moderate importance over drainage proximity; thus, a value of 2 is assigned. It is, however, of moderate importance compared to watershed slopes with a scale of 3. It is essentially more important than soil infiltration capacity, soil type, and road proximity, assigning a value of 5.

Table 12. Pairwise comparison matrix for the six criteria basis of the RB location prospecting by AHP.

Factors	LULC	Drainage Proximity	Watershed Slope	Infiltration Capacity	Soil Type	Road Proximity
LULC	1	2	3	5	5	5
Drainage Proximity	1/2	1	3	4	5	5
Watershed Slope	1/3	1/3	1	5	5	5
Infiltration Capacity	1/5	1/4	1/5	1	1	2
Soil Type	1/5	1/5	1/5	1	1	2
Road Proximity	1/5	1/5	1/5	1/2	1/2	1
Sum	2.43	3.98	7.60	16.50	17.50	20.00

Drainage proximity is moderately more important than watershed slope, with a scale of 3. It is, however, in between moderate to essentially strong importance compared to infiltration capacity and is of strong importance compared to soil type and road proximity, assigning values of 4 and 5, respectively. Watershed slope is essentially of strong importance than infiltration capacity, soil type, and road proximity. Thus, a value of 5 is assigned.

Infiltration capacity is of equal relative importance with its corresponding soil type with a value of 1 and of intermediate importance between equal to moderate importance compared to road proximity, having a scale of 2. Soil type is of intermediate importance, ranging from equal to moderate prominence with road proximity with a value of 2. The rest are reciprocals of already assigned relative values.

Table 13. Normalized pairwise comparison matrix for the six criteria basis of the RB location prospecting.

Factors	LULC	Drainage Proximity	Watershed Slope	Infiltration Capacity	Soil Type	Road Proximity	Sum	Criteria Weights	
LULC	0.4110	0.5021	0.3947	0.3030	0.2857	0.2500	2.146	0.3578	36
Drainage Proximity	0.2055	0.2510	0.3947	0.2424	0.2857	0.2500	1.629	0.2716	27
Watershed Slope	0.1370	0.0837	0.1316	0.3030	0.2857	0.2500	1.191	0.1985	20
Infiltration Capacity	0.0822	0.0628	0.0263	0.0606	0.0571	0.1000	0.389	0.0648	6
Soil Type	0.0822	0.0502	0.0263	0.0606	0.0571	0.1000	0.376	0.0627	6
Road Proximity	0.0822	0.0502	0.0263	0.0303	0.0286	0.0500	0.267	0.0446	5
							SUM	1.0000	100

The normalized pairwise matrix in Table 13 shows the final weightage of each criterion. Land cover is the highest influencing criterion with 36% weight, followed by drainage proximity with 27%, watershed slope with 20%, infiltration capacity, and soil type with an equal weight of 6%, and road proximity is the least influential with a weighted value of 5%. Environmental factors are the most significant in the decision-making framework in retarding basin location prospecting, especially the usage and covering of the area.

The normalized matrix has a consistency ratio of 0.06, which falls within the critical acceptable inconsistency value of less than 0.10 [26]. Results reveal that the degree of inconsistency of the judgments is at 6% and is sufficient enough to be used for further analysis. Thus, the judgment on evaluating the criteria's relative importance is reliable

and adequate for weighted overlay generation with all necessary data summed up in Table 14.

Table 14. Summary of criteria, sub-criteria, suitability level, preference value, and weightage percentage.

Criteria	Sub-criteria	Level of Suitability	Preference Value	Weight (%)
LULC	Rangeland	Highly Suitable	5	36
	Agricultural Land	Moderately	4	
	Forestland	Suitable	3	
	Barren Land	Suitable	2	
	Urban/Built-up	Not Suitable	0	
Proximity to drainage	0<distance≤100	Highly Suitable	5	27
	101<distance≤200	Moderately Suitable	4	
	201<distance≤300		3	
	301<distance≤400	Suitable	2	
	401<distance≤500	Not Suitable	1	
	>500		0	
Watershed slope	0 < slope ≤ 2	Highly Suitable	5	20
	2 < slope ≤ 4	Moderately Suitable	4	
	4 < slope ≤ 6		3	
	6 < slope ≤ 8	Suitable	2	
	8 < slope ≤ 10	Not Suitable	1	
	slope > 10		0	
Infiltration capacity	0 < inf ≤ 1	Highly Suitable	0	6
	1 < inf ≤ 2	Moderately Suitable	1	
	2 < inf ≤ 3		2	
	3 < inf ≤ 4	Suitable	3	
	4 < inf ≤ 5	Not Suitable	4	
	inf > 5		5	
Soil type	Sand	Highly Suitable	5	6
	Sandy loam	Moderately	4	
	Silty loam	Suitable	3	
	Clay loam	Suitable	2	
	Clay	Not Suitable	1	
Proximity to road	0<distance≤50	Highly Suitable	5	5
	50<distance≤100	Moderately Suitable	4	
	100<distance≤150		3	
	150<distance≤200	Suitable	2	
	> 200	Not Suitable	1	

3.2 Weighted overlay

Fig. 5 shows the six thematic maps after reclassification where 5(a) is the reclassified LULC, 5(b) is the reclassified drainage proximity, 5(c) is the reclassified watershed slope, 5(d) is the reclassified infiltration capacity, 5(e) is the reclassified soil type, and 5(f) is the reclassified road accessibility. With the calculated criteria weights, the thematic maps (Fig. 5) were integrated into an overlay map (Fig. 6), identifying areas of high suitability for retarding basin placement.

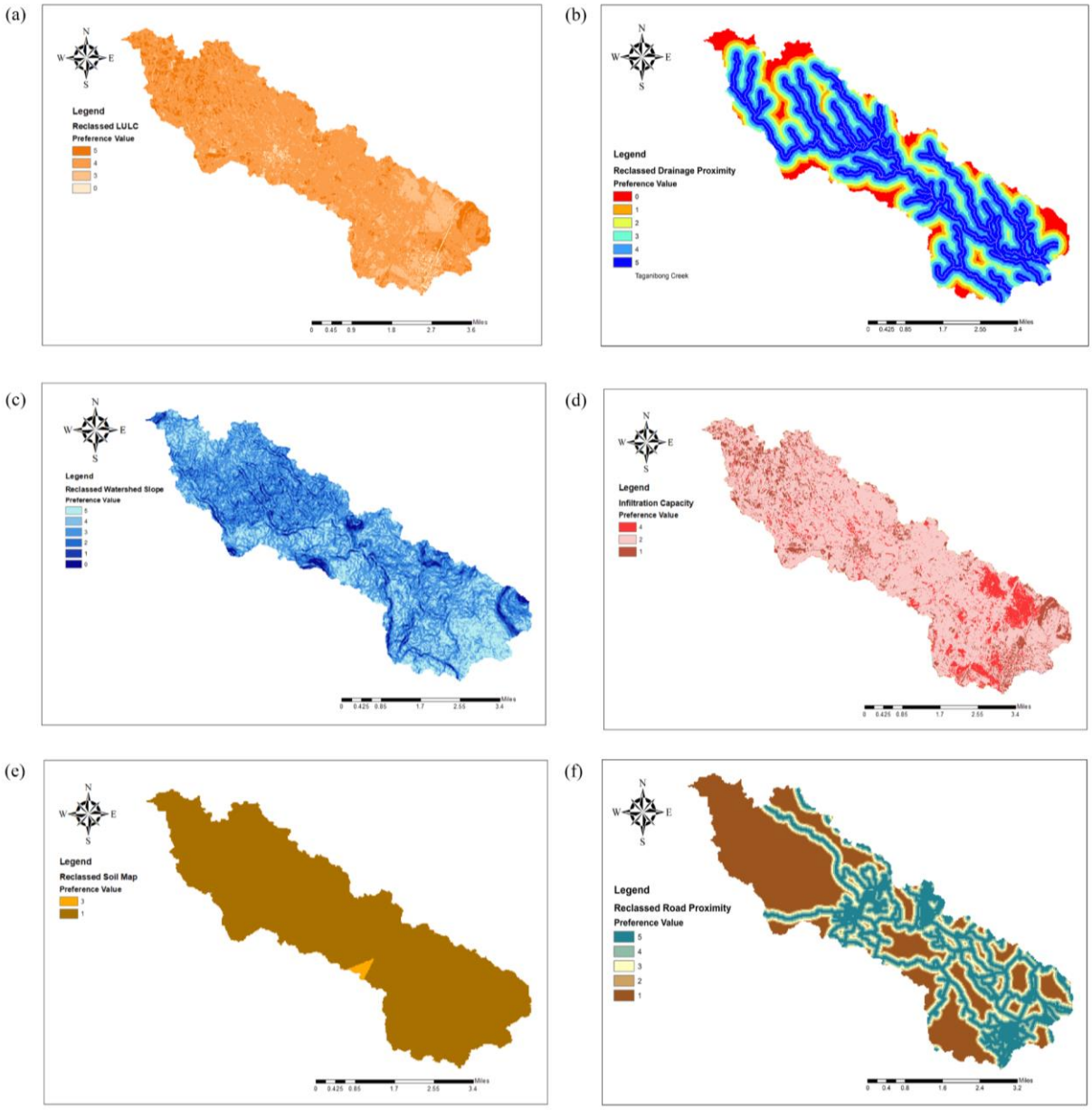

Fig. 5. Thematic Maps (a) LULC, (b) Drainage Proximity, (c) Watershed Slope, (d) Soil Infiltration, (e) Soil Type, (f) Road Accessibility

Fig. 6 shows the areas that fall into each zone of suitability while Table 15 provides the numerical details. About 2.00% of the area falls on a restricted zone, suggesting no retarding basin is placed as it comprises built-up infrastructures. The rest of the restricted area percentage is attributed to its distance from the stream link and roads, steep slopes, low to no soil infiltration rates, clayey soils, and distance from the road. Suitable areas account for 39.58%, while moderately suitable locations comprise the highest area percentage of 57.76%, about 17.25, and 25.17 km^2, respectively. With the least percentage, highly suitable areas for retarding basin placement accounts for 0.67% with an area of 0.29 km^2. The highly suitable zone is relatively less in the accumulated area as little land has fulfilled all the criteria, demonstrating the best location by its environmental, physical, and accessibility features.

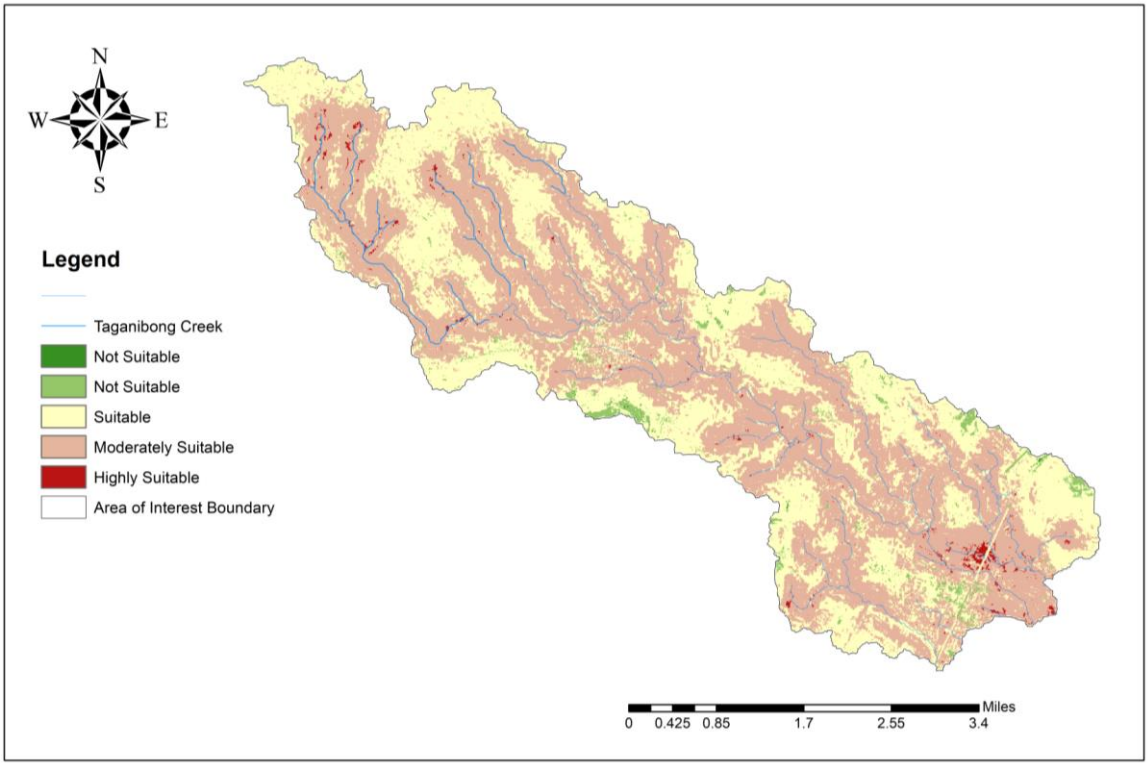

Fig. 6. Weighted overlay map

Table 15. Suitability levels area on overlay map

Suitability Level	Area in sq. km	Area in percentage
Not Suitable	0.87	2.00
Suitable	17.25	39.58
Moderately Suitable	25.17	57.76
Highly Suitable	0.29	0.67
TOTAL	43.58	100.0

3.3 Location prospects

Areas inundated in the past floods with no housing are suitable locations for retarding basins [27]. Although the overlay map locates suitable areas for a retarding basin, the use of hydrodynamics simulations can mostly verify inundated parts of the study area.

Based on the past flood, the onslaught of Bagyong Pablo last December 4, 2012, a 6-hour 25-year storm, with a 4% exceedance probability of such magnitude to occur every year, is simulated and is used for the validation of the overlaid suitability map with an RMSE of 0.2863, suggesting that the model can relatively predict flood depths. Based on the overlay map, five locations are under high suitability zones and have been inundated in the past flood simulation.

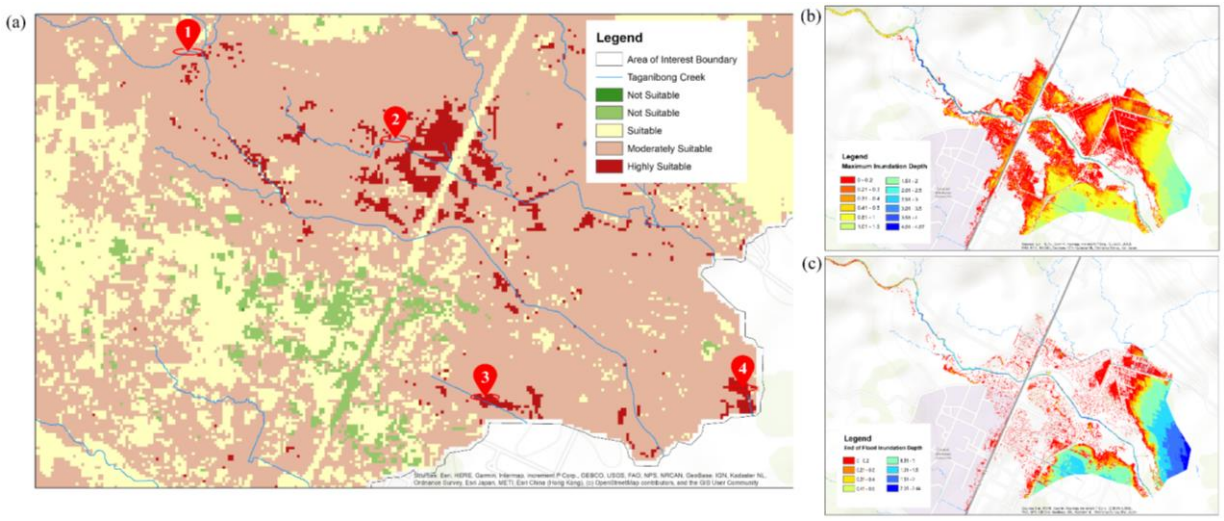

Fig. 7. Retarding basin high suitability zones 1-4 based on the (a) overlay map, in (b) maximum, and (c) end of the simulated 6hr-25yr flood

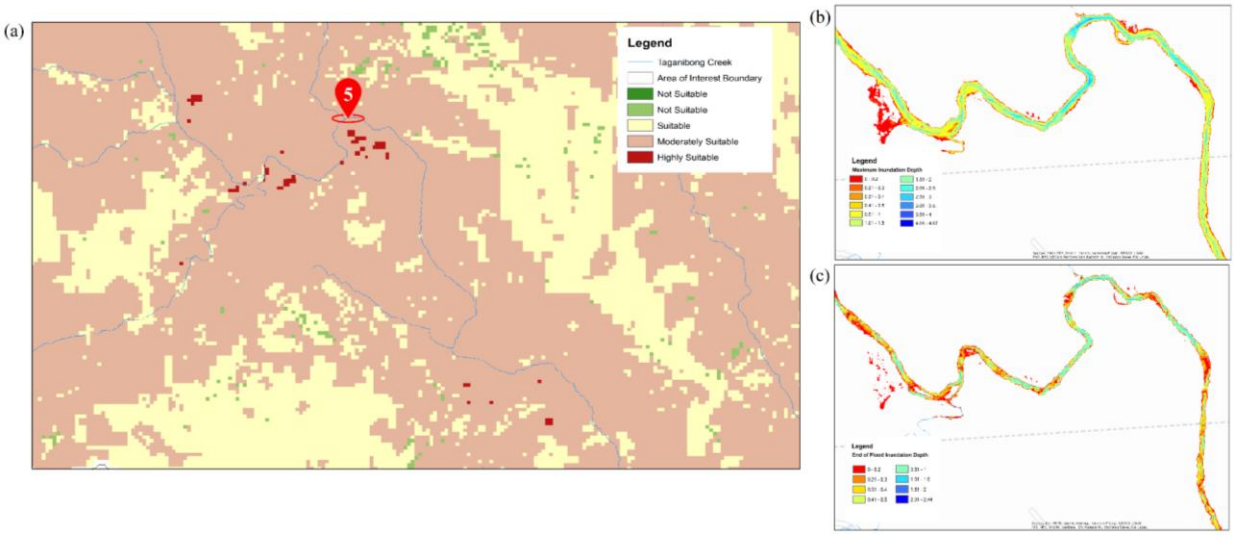

Fig. 8. Retarding basin high suitability zone 5 based on the (a) overlay map, in (b) maximum, and (c) end of the simulated 6hr-25yr flood

Concentrations of high suitability are visible at five locations. With relatively flat slopes of less than 2 degrees at lower elevations, locations 3 and 4 are likely to be inundated, reaching up to a range of 1.51 to 2.00 meters flood depth as shown in Fig. 7b. Depths greater than 1.5 m are considered high hazard [28]. Contrary to the proximity of suitable zones to drainage, these two locations are defiant, and reducing peak time flows may be difficult as they close in with the study area's outlet.

With green pixelated dense settlements at the right bank of the creek, specifically on the university campus, the overlay map restricts these areas for retarding basin placement despite being inundated on the simulation. On the other side of the bank, at location 2, high suitability is reflected as rangeland is detected. Inundated areas are reflected on the overlay map as highly suitable pixels, with sparse, minimal overflows in location 1 and more concentrated inland spills further downstream with the highest inundation depth range of 0.51 to 1.00 m, as shown in Fig. 7b, denoting a medium hazard flood.

Meanwhile, Fig. 8a shows the overlay map further upstream of the study area at location 5 with few reasonable spots of high suitability. Several spills of flow discharge are also identifiable along the river on the maximum flood simulation.

With the aid of GIS-based multi-criteria decision analysis and validation through flood inundation map, shown in Fig. 9 and Table 16 are three upstream retarding basin site prospects and their coordinates, which include areas in Litig, Diversion Canal, and in CMU Dairy Project denoted as RB1, RB2, and RB3, respectively.

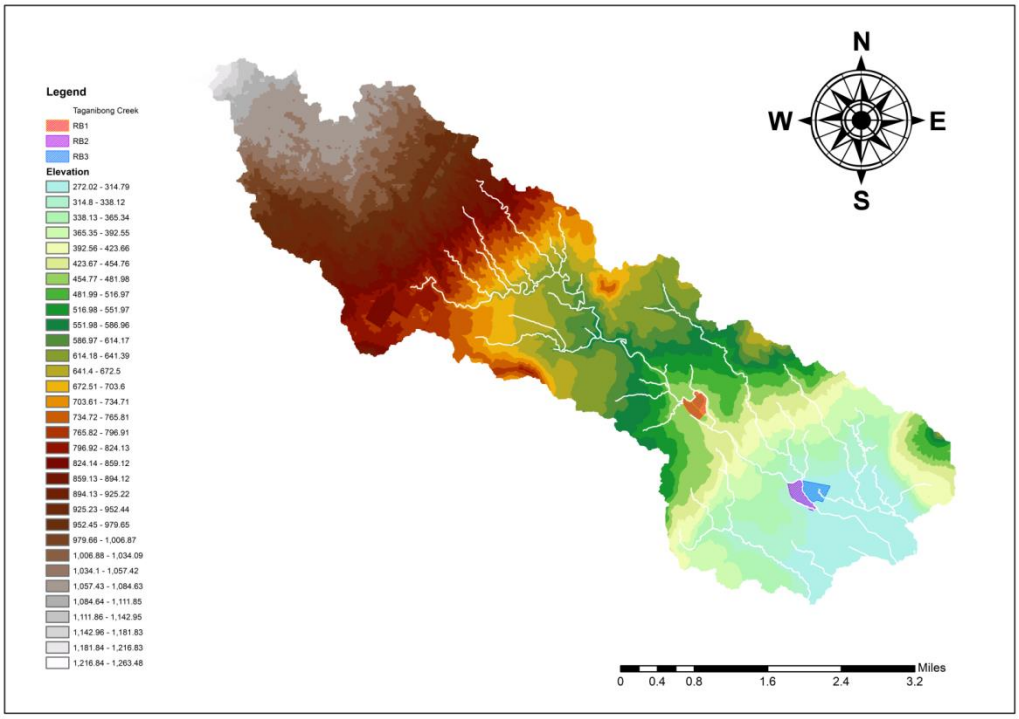

Fig. 9. Retarding basin area locations.

Table 16. Retarding basin prospect locations

	RB1	RB2	RB3
River	Taganibong Creek	Taganibong Creek	Taganibong Creek
Right Bank/Left Bank	Right Bank	Right Bank	Left Bank
Location	7°52'6.77"N 125° 2'47.99"E	7°52'6.95"N 125° 2'54.86"E	7°53'21.70"N 125° 1'18.05"E

3.4 Pre- and Post-Retardation Hydrologic Analysis using HEC-HMS

3.4.1 Model Calibration and Validation

Using precipitation and discharge data from the rainfall event on December 4, 2012, the uncalibrated model generated a flow hydrograph displayed in Fig. 10(a) with a peak discharge of 25.4 cu.m./s and a runoff volume of 621.7 (1000 cu.m.). The hydrograph peaked at 15:00 PM. These results show notable differences from the observed flow hydrograph in Fig. 10(a), which records a peak discharge of 13.5 cu.m./s and a runoff volume of 367.4 (1000 cu.m.). However, the peaking times of the predicted and observed hydrographs differ by 30 minutes. Model predictions prior to calibration, when compared to the observed flow data, were assessed and had an NSE of -3.433, PBIAS of 68.81%, and RSR of 2.1. These performance rating values suggest that the model inadequately predicted the streamflow hydrograph resulting from the input rainfall event [25].

Initially, the initial abstraction (Ia) to maximum retention (S) ratio in the SCS curve number loss model was set at 0.2 [35]. Using the optimization tool in HEC-HMS, this ratio was recalibrated through iterative adjustments, resulting in a reduction from 0.2 to 0.05. This recalibrated ratio aligns with the findings of Perodes and Fornis [36], who conducted rainfall-runoff event analysis for a nearby watershed and determined an initial abstraction ratio of 0.03. The curve number values for each subbasin were optimized by a factor of 0.7 of their identified initial values. The lag time to time of concentration ratio was increased from 0.6 to 0.9 to address the difference in times to peak between observed and predicted hydrographs. The recalibrated model predicted a peak discharge shown in Fig. 10(b) of 11.8 cu.m./s and a runoff volume 334.2 (1000 cu.m.). The projected hydrograph peak occurred at 14:00 PM. When comparing the observed and predicted values, there is a difference of 1.7 cu.m./s in peak discharge rates and 33.2 cu.m. in runoff volume.

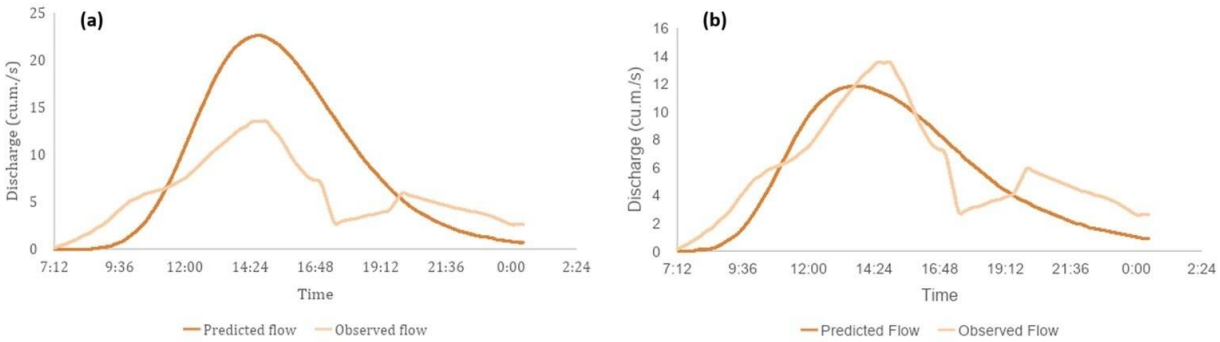

Fig. 10. Observed discharge on December 4, 2012 vs. the predicted discharge by the (a) initial, and (b) optimized parameters.

When assessed against observed discharge, model predictions of the calibrated model were rated with an NSE coefficient of 0.718, an RSR of 0.5, and a PBIAS of -9.19, as summarized in Table 17. An NSE coefficient between 0.65 and 0.75 is considered good, an RSR equal to 0.50, and a PBIAS less than ±10 indicate that the model performed very well and satisfactorily predicted discharge values [25].

Table 17. Model predictions and model performance rating for initial and optimized parameters

	Date	Observed hydrograph	Predicted hydrograph (Initial)	Predicted hydrograph (Optimized)
Peak Discharge (cu.m./s)	12/04/2012	13.5	25.4	11.8
Runoff Volume (1000 cu.m.)	12/04/2012	367.4	621.7	334.2
Time		14:30 PM	15:00 PM	14:00 PM
Nash-Sutcliffe efficiency (NSE)			-3.433	0.718
Root mean square-standard deviation ratio (RSR)			2.1	0.5
Percent bias (PBIAS)			68.81	-9.19

The calibrated model was used for validation of the model. The August 16, 2016-rainfall data was used to simulate discharges and is compared to its observed discharges. The model, as shown in Fig. 11 and as summarized in Table 18, projected a peak discharge of 23.5 cu.m./s and a 507 (1000 cu.m.) runoff volume. These values exhibit differences from the observed peak discharge and runoff volume by 8.3 cu.m./s and 22.7 (1000 cu.m.), respectively.

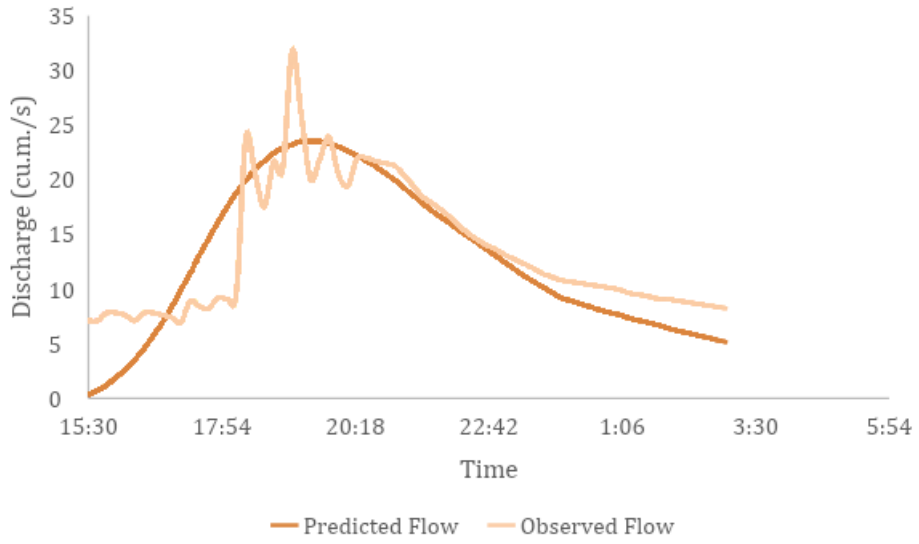

Fig. 11. Observed discharge on August 16, 2016 vs. the predicted discharge by recalibrated parameters.

An NSE coefficient of 0.685 and an RSR of 0.6 are considered good and satisfactory, while a PBIAS of -4.85 indicates that the model is very good at predicting discharge values [25].

Table 18. Model predictions and model performance rating after validation.

	Date	Observed hydrograph	Predicted hydrograph
Peak Discharge (cu.m./s)	08/16/2016	31.8	23.5
Runoff Volume (1000 cu.m.)	08/16/2016	529.7	507
Time		19:10 PM	19:30 PM
Nash-Sutcliffe efficiency (NSE)		0.685	
Root mean square-standard deviation ratio (RSR)		0.6	
Percent bias (PBIAS)		-4.85	

3.4.2 Discharge Simulations without Retarding Basin

After determining that the calibrated and validated model is good enough for simulating rainfall-runoff scenarios, discharge simulations were first performed without a retarding basin for 3-hour, 6-hour, 10-hour and 24-hour rainfall durations at return periods 10, 25, 50, and 100 years which are summarized in Table 19.

Table 19. Watershed response to design storms without retarding basin.

Duration (hour)	Return Period (year)	Peak Discharge (cu. m/s)	Volume (1000 cu.m.)	Time of Peak
3	10	23.3	564.1	13:15
	25	29.6	717.7	13:15
	50	35.9	871	13:15
	100	42.3	1025.6	13:15
6	10	31.3	770.2	15:15
	25	39.1	962.9	15:15
	50	47.2	1162.5	15:15
	100	55.3	1362.6	15:15

10	10	35.9	927.1	17:15
	25	44.5	1145.3	17:15
	50	53.6	1377.8	17:15
	100	62.6	1609.8	17:15
24	10	42.8	1211.1	00:15
	25	52.5	1473.4	00:15
	50	62.8	1764.1	00:15
	100	73.1	2052.9	00:15

At the 3-hour duration, the outlet discharge and total runoff volume are as follows: 23.3 cu.m./s with 564.1 (1000 cu.m.) for the 10-year return period, 29.6 cu.m./s with 717.7 (1000 cu.m.) for the 25-year return period, 35.9 cu.m./s with 871 (1000 cu.m.) for the 50-year return period, and 42.3 cu.m./s with 1025.6 (1000 cu.m.) for the 100-year return period.

For the 6-hour duration, the outlet discharge and total runoff volume are: 31.3 cu.m./s with 770.2 (1000 cu.m.) for the 10-year return period, 39.1 cu.m./s with 962.9 (1000 cu.m.) for the 25-year return period, 47.2 cu.m./s with 1162.5 (1000 cu.m.) for the 50-year return period, and 55.3 cu.m./s with 1362.6 (1000 cu.m.) for the 100-year return period.

Moving to the 10-hour duration, the outlet discharge and total runoff volume are: 35.9 cu.m./s with 927.1 (1000 cu.m.) for the 10-year return period, 44.5 cu.m./s with 1145.3 (1000 cu.m.) for the 25-year return period, 53.6 cu.m./s with 1377.8 (1000 cu.m.) for the 50-year return period, and 62.6 cu.m./s with 1609.8 (1000 cu.m.) for the 100-year return period.

Finally, at the 24-hour duration, the outlet discharge and total runoff volume are: 42.8 cu.m./s with 1211.1 (1000 cu.m.) for the 10-year return period, 52.5 cu.m./s with 1473.4 (1000 cu.m.) for the 25-year return period, 62.8 cu.m./s with 1764.1 (1000 cu.m.) for the 50-year return period, and 73.1 cu.m./s with 2052.9 (1000 cu.m.) for the 100-year return period.

The peak times occur at 13:15 PM (3-hour), 15:15 PM (6-hour), 17:15 PM (10-hour), and 00:15 AM (24-hour) with different return periods.

3.4.3 Discharge Simulations with Retarding Basin

The recommended design storm for a PHRC-2 classification of dam or reservoir structures based on the guidelines established by the National Irrigation Administration [29] is a 10-year return period. To determine the area-elevation data essential for incorporating the retarding basin into the HEC-HMS software, the total runoff volume over a 6-hour duration and a 10-year return period served as the basis of design.

The area-elevation data employed for the storage method in the outflow structure within the reservoir routing was determined at three potential locations: RB1, RB2, and RB3, as illustrated in Fig. 9. A total runoff volume of 770,000 cu.m. with a 0.6 m freeboard was used as the basis for designing the retarding basin. Subsequently, runoff simulations for various design storms were conducted and summarized in Table 20, 21, and 22, with corresponding runoff hydrographs at a 10-year return period incorporating the subbasins at 3-hour, 6-hour, 10-hour, and 24-hour duration displayed in Fig. 12. The detailed results for the runoff simulations and their corresponding hydrographs, considering the presence of a retarding basin, for 25, 50, and 100-year return periods with 3-hour, 6-hour, 10-hour, and 24-hour durations, are provided in the supplementary file.

Three new basin models were developed in HEC-HMS, incorporating RB1, RB2, and RB3, to simulate the runoff resulting from 3-hour, 6-hour, 10-hour, and 24-hour rainfall events with 10-year, 25-year, 50-year, and 100-year return periods.

Table 20. Watershed response to design storms with RB1 at 10-year return period.

Duration (hour)	Peak Discharge (cu. m/s)	Volume (1000 cu.m.)	Time of Peak
3	5.6	173.0	14:45
6	7.7	231.1	16:45
10	9.3	265.2	19:45

24	11.3	338.1	2:15

In the presence of RB1, the time of peak was delayed by 1 hour and 30 minutes at various time durations compared to the time of peak when no retarding basin was incorporated. RB1 effectively intercepted Reach 3, where runoff accumulated from Subbasins 1, 2, 3, 4, 5, 6, 7, and 24—tributary areas encompassing approximately 16.5722 sq. km.

Table 21. Watershed response to design storms with RB2 at 10-year return period.

Duration (hour)	Peak Discharge (cu. m/s)	Volume (1000 cu.m.)	Time of Peak
3	5.2	157.1	15:15
6	7.2	208.9	17:15
10	8.6	237.3	19:45
24	10.4	300.6	2:45

With the integration of RB2, the timing of the peak was deferred by 2 hours at various durations compared to the peak time without the implementation of a retarding basin. RB2 effectively intercepted Reach 2, where runoff collected from Subbasins 1, 2, 3, 4, 5, 6, 7, 10, and 24—tributary areas covering approximately 20.0671 sq. km.

Table 22. Watershed response to design storms with RB3 at 10-year return period.

Duration (hour)	Peak Discharge (cu. m/s)	Volume (1000 cu.m.)	Time of Peak
3	20.1	428.4	13:00
6	26.7	590.1	15:00
10	30.4	723.9	17:00
24	36.0	954.2	0:00

With the integration of RB3, the time of peak was advanced by 15 minutes at various time durations compared to the time of peak when no retarding basin was implemented. RB3 effectively intercepted Reach 8, where runoff accumulated from Subbasins 8, 10, and 23—tributary areas encompassing approximately 7.203 sq. km.

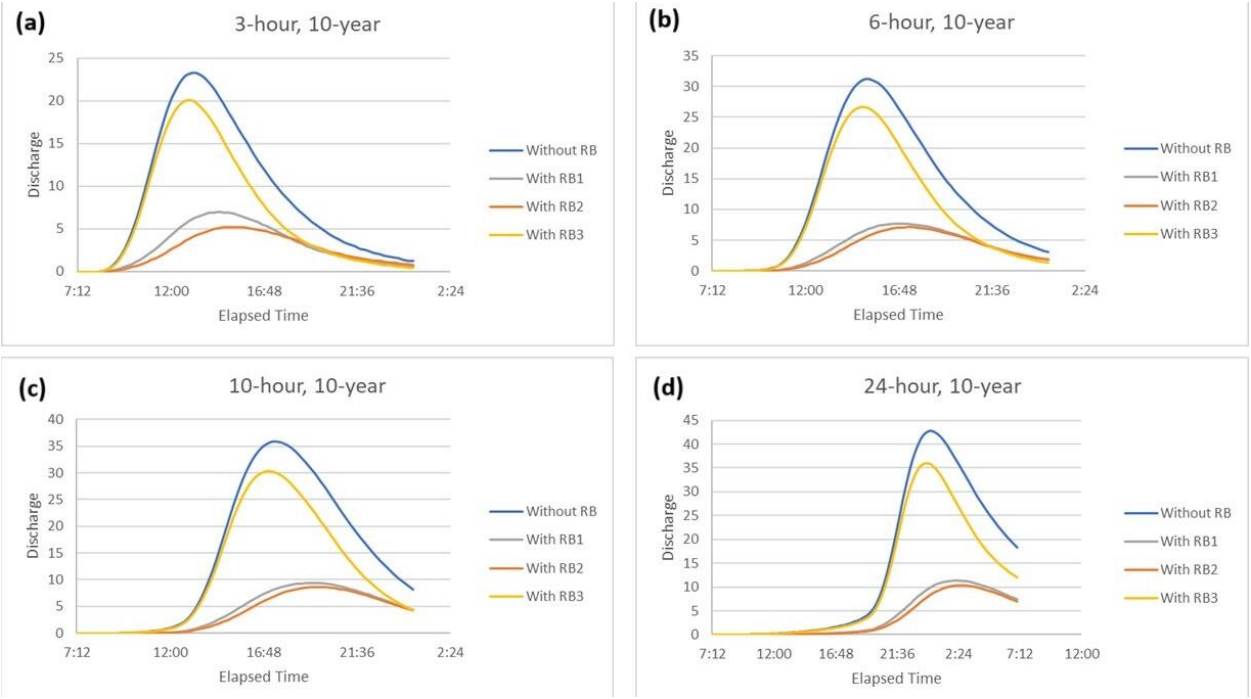

Fig. 12. Model response with and without retarding basin in 10-year storm at (a) 3-hour, (b) 6-hour, (c) 10-hour, and (d) 24-hour duration.

3.5 Site Selection

Following simulations of discharges at three prospective locations with precipitation for various return periods and durations, a percentage reduction was calculated, both with and without the presence of a retarding basin. The decision hinges on the percentage reduction of peak discharges achievable by incorporating a retarding basin at the three prospective locations, as determined by GIS-based multi-criteria decision analysis.

The presence of a retarding basin creates a significant decrease in peak discharge at different locations, as shown in Table 23. Among the three retarding basins employed on the basin model, RB2 governs in substantial reduction of peak discharge. At a 10-year return period, RB2 creates approximately a 77% decrease in peak discharge in 3-hour and 6-hour duration. Approximately 76% and 75% decrease in peak discharge for 10-hour and 24-hour duration, respectively. Similarly, RB1 creates approximately a 76% decrease in peak discharge at a 10-year return period in a 3-hour duration, a 75% decrease in a 6-hour duration, 73% in a 10-hour duration, and 72% in a 24-hour duration. Lastly, RB3 creates approximately a 13% decrease in peak discharge in a 3-hour duration at a 10-year return period, a 14% decrease in a 6-hour duration, and a 15% 10-hour and 24-hour duration. However, for each respective retarding basin, the percent reduction of peak discharge is approximately the same across different return periods for each duration. Detailed data on the percent reduction of peak discharge, considering the three retarding basins for 25, 50, and 100-year return periods with 3-hour, 6-hour, 10-hour, and 24-hour durations, are provided in the supplementary file.

Table 23. Effect of the implementation of a retarding basin on the discharge peaks at 10-year return period.

Duration (hour)	Percent reduction of peak discharge (%)		
	RB1	RB2	RB3
3	76.07	77.68	13.73
6	75.08	77.00	14.70
10	73.43	76.04	15.32
24	72.64	75.70	15.89

To assess the hydraulic response of the vicinity with the addition of the retarding basin, a 2D unsteady flow model was developed using HEC-RAS (Fig. 13). The hydrograph utilized for the unsteady state data was the simulated inflow at 6-hour, 10-year without the presence of a retarding basin. Following terrain modifications, considering a total runoff volume of 770,000 cu.m., the simulation results indicated that the retarding basin effectively stored water, leading to a reduction in discharge at the outlet portion.

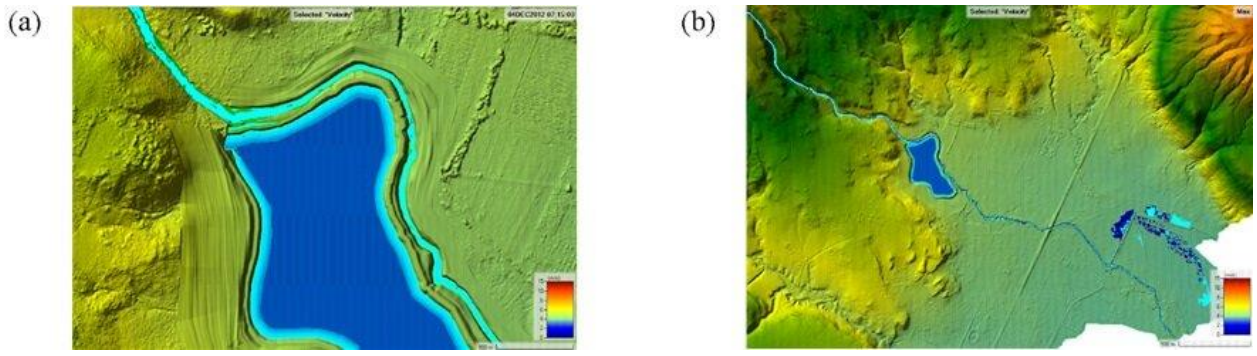

Fig. 13. HEC-RAS Simulation (a) Presence of retarding basin projecting static velocity arrows, and (b) Zoom out view of retarding basin at 6-hour duration at 10-year return period.

4. CONCLUSION

Retarding basin location prospecting requires multiple criteria, weighted by AHP, and spatially generated by geographic information system. The highest influencing criterion is land use/cover (36%), followed by drainage proximity (27%), watershed slope (20%), infiltration capacity and soil type (6%), and road proximity (5%). Consistency ratio of 0.06 implies the criteria weights' reliability to define the suitability map by weighted overlay. The coherence of spatially identified high-suitability pixels in the overlay and flood inundation map is visible at three upstream locations throughout the watershed.

Site selection among site prospects involves a pre- and post-retardation analysis using a validated hydrological model for Taganibong Creek. The model achieved favorable performance ratings, with an NSE of 0.718, an RSR of 0.5, and a PBIAS of -9.1 during calibration, and an NSE of 0.685, an RSR of 0.6, and a PBIAS of -4.85 during validation. Hence, this indicates an accurate prediction of the watershed response at the outlet due to rainfall.

The validated hydrological model simulates the 6-hour 10-year storm to determine the retarding basin volume capacity. To account for the presence of the retarding basin, the outflow structure routing method was employed, along with the corresponding storage method requiring area-elevation paired data.

The validated hydrological model simulated discharges with pre- and post-retardation conditions in three locations in a 3-hour, 6-hour, 10-hour, and 24-hour storm duration. Significant decreases in peak discharge were observed in RB1 (75%), RB2 (77%), and RB3 (13%). Additionally, the presence of the retarding basin induced a delay in peak time by 1 hour and 30 minutes for RB1, 2 hours for RB2, and an advancement by 15 minutes for RB3. Consequently, the most suitable retarding basin location is at RB2. Thus, retarding basin implementation at RB2 can effectively reduce peak discharges and delay peak times, demonstrating its suitability for flood mitigation in the watershed.

Broadening the range of multi-criteria decision analysis techniques is highly recommended for a more coherent judgment. Moreover, it is recommended that advanced rainfall monitoring techniques and equipment be used for convenient and precise discharge measurements to further improve the hydrological model's accuracy. This study's findings can contribute to future flood mitigation efforts at Central Mindanao University. The methodology used, from site search to site selection, can serve as a valuable approach for researchers dealing with flood-related challenges.

Author Contributions: A.A.V. and K.Q.A. contributed equally to this study, including the conceptualization, data collection, analysis, and interpretation of the results. J.R.P. provided guidance and oversight throughout the project and contributed to the study's design, methodology, and critical revisions of the manuscript. All authors discussed the results, contributed to the final manuscript, and approved its submission.

Funding: This research received no external funding.

Data Availability Statement: The data used in this study are available from the authors upon reasonable request.

Acknowledgments: The researchers express deep gratitude to Althia Jane A. Divino, Ma. Fatima Theresa B. Abayato, and the faculty of the Department of Civil Engineering, Central Mindanao University. Above all, to Almighty God, who sustained them through challenges and weaknesses.

Conflicts of Interest: The authors declare no conflicts of interest.

5. REFERENCES

Abeysingha, N., Singh, M., Sehgal, V. K., & Srinivasan, R. (2015). Assessment of water yield and evapotranspiration over 1985 to 2010 in the Gomti river basin in India using... ResearchGate. https://www.researchgate.net/publication/304659569_Assessment_of_water_yield_and_evapotranspiration_over_1985_to_2010_in_the_Gomti_River_basin_in_India_using_the_SWAT_model

Aidinidou, M. T., Kaparis, K., & Georgiou, A. C. (2023). Analysis, prioritization and strategic planning of flood mitigation projects based on sustainability dimensions and a spatial/value AHP-GIS system. Expert Systems With Applications, 211, 118566. https://doi.org/10.1016/j.eswa.2022.118566

Bas, J. L. (2019). A GIS-Based multi-criteria decision framework for selecting suitable locations of sustainable flood retention basins at the watershed scale: The case of the upper subcatchments of the Butuanon river watershed [Thesis, University of San Carlos].

Bruno, A. G. (2016). Integrating GIS with landuse decision making: The case of Central Mindanao University, Philippines [Thesis, Central Mindanao University].

Cabrera, J., & Lee, H. S. (2019). Flood-Prone area assessment using GIS-Based multi-criteria analysis: A case study in Davao Oriental, Philippines.

Central Mindanao University. (2012). Annual report 2012.

Chen, Y. (2022). Flood hazard zone mapping incorporating geographic information system (GIS) and multi-criteria analysis (MCA) techniques. Journal of Hydrology, 612, 128268. https://doi.org/10.1016/j.jhydrol.2022.128268

Darwish, K. (2023). GIS-Based multi-criteria decision analysis for flash flood hazard and risk assessment: A case study of the eastern of Minya area, Egypt. Environmental Sciences Proceedings, 25(87).

Gabule, J. (2016). Geomorphologic characteristics and hydrologic features of Taganibong creek [UndergraduateThesis].

HEC-HMS User's Manual. (n.d.). https://www.hec.usace.army.mil/confluence/hmsdocs/hmsum/latest

Iso-specific Coefficient, Attachment 4.4 of "Specific Discharge Curve, Rainfall Intensity Duration Curve, Isohyet of Probable 1-day Rainfall", FCSEC, March 2003.

Isohyet of Probable 1-Day Rainfall, Attachment 4.5 of "Specific Discharge Curve, Rainfall Intensity Duration Curve, Isohyet of Probable 1-day Rainfall", FCSEC, March 2003.

JICA. (n.d.). Chapter 2. Results of feasibility study on the priority project as structural flood mitigation measures.

Lee, J. G., Selvakumar, A., Alvi, K., Riverson, J., Zhen, J., Shoemaker, L., & Lai, F. (2012). A watershed-scale design optimization model for stormwater best management practices. Environmental Modelling & Software, 37, 6–18. https://doi.org/10.1016/j.envsoft.2012.04.011

Lee, Y., Keum, H., Han, K., & Hong, W. (2020). A hierarchical flood shelter location model for walking evacuation planning. Environmental Hazards, 20(4), 432–455. https://doi.org/10.1080/17477891.2020.1840327

Lor, A. J. A. (2013). Runoff rate determination of Taganibong watershed in Bukidnon using unit hydrograph [Undergraduate Thesis].

Malczewski, J. (1999). GIS and multi criteria decision analysis. Computers & Geosciences (1st ed., Vol. 26, p. 392).

Malczewski, J., & Rinner, C. (2015). Multicriteria decision analysis in geographic information science. Advances in Geographic Information Science. https://doi.org/10.1007/978-3-540-74757-4

National Statistics Office. (1995). Provincial Profile Bukidnon (2nd edition) (ISBN 971-562-497-9).

Ngo, T. T., Yoo, D. G., Lee, Y. S., & Kim, J. H. (2016). Optimization of upstream detention reservoir facilities for downstream flood mitigation in urban areas. Water, 8(7), 290. https://doi.org/10.3390/w8070290

NIA-General Guidelines & Criteria for Planning, Design, Construction, Operation and Maintenance of Reservoir Dams/1st Edition (2019)/jrp. (2019).

Ogania, J., Puno, G., Alivio, M., & Taylaran, J. (2019). Effect of digital elevation model's resolution in producing flood hazard maps. Global Journal of Environmental Science and Management, 5(1), 95–106. https://doi.org/10.22034/gjesm.2019.01.08

Palmate, S. S., & Pandey, A. (2020). Effectiveness of best management practices on dependable flows in a river basin using hydrological SWAT model. In Water science and technology library (pp. 335–348). https://doi.org/10.1007/978-3-030-58051-3_22

Perodes, J. R., & Fornis, R. L. (2024). Determining the Initial Abstraction Ratio of the Upper Sawaga Watershed, Bukidnon, Philippines. CMU Journal of Science, 28(1), 70.

RIDF of Selected Synoptic PAGASA Station, Attachment 4.3 of "Specific Discharge Curve, Rainfall Intensity Duration Curve, Isohyet of Probable 1-day Rainfall", FCSEC, March 2003.

Riverson, J., Zhen, J., Shoemaker, L., & Lai, F. (2004). Design of a decision support system for selection and placement of BMPs in urban watersheds. Critical Transitions in Water and Environmental Resources Management. https://doi.org/10.1061/40737(2004)40

Saaty, T. L. (1977). A scaling method for priorities in hierarchical structures, Journal of Mathematical Psychology, 15, pp 234281.

Saaty, T. L. (1980). The analytical hierarchy process. McGraw-Hill, New York.

Saaty, T. L. (1988). What is the analytic hierarchy process? 1988. doi:10.1007/978-3-642-83555-1_5.

Saragih, D. F., Ahamad, M. S., & Abdullah, R. (2020). Chapter application of geographic information systems (GIS) in the multi criteria site selection of retention pond for urban rainwater management. ResearchGate. https://doi.org/10.1007/978-3-030-32816-0_20

Saragih, D. F., Ahamad, M. S. S., & Abdullah, R. (1970). Application of geographic information systems (GIS) in the multicriteria site selection of retention pond for urban rainwater management. SpringerLink.

Shi, Z., Chen, L., Fang, N., Qin, D., & Cai, C. (2009). Research on the SCS-CN initial abstraction ratio using rainfall-runoff event analysis in the Three Gorges Area, China. Catena, 77(1), 1–7. https://doi.org/10.1016/j.catena.2008.11.006

Sholihah, Q., Kuncoro, W., Wahyuni, S., Suwandi, S. P., & Feditasari, E. D. (2020). The analysis of the causes of flood disasters and their impacts in the perspective of environmental law. IOP Conference Series. Earth and Environmental Science, 437(1), 012056. https://doi.org/10.1088/1755-1315/437/1/012056

Sisman, S., & Aydınoğlu, A. Ç. (2020). Using GIS-based multi-criteria decision analysis techniques in the smart cities. The International Archives of the Photogrammetry, Remote Sensing and Spatial Information Sciences, XLIV-4/W3-2020, 383–389.

Thome, A. C. G. (2012). SVM classifiers – Concepts and applications to character recognition. In InTecheBooks. https://doi.org/10.5772/52009

Wang, J., Jing, Y., Zhang, C., & Zhao, J. (2009). Review on multi-criteria decision analysis aid in sustainable energy decision making. Renewable & Sustainable Energy Reviews, 13(9), 2263–2278. https://doi.org/10.1016/j.rser.2009.06.021